

Kinetic-Energy Distributions and the Correlation of Anisotropy and Asymmetry in the 4-MeV Neutron-Induced Fission of U^{235}

S. S. KAPOOR, D. M. NADKARNI, R. RAMANNA, AND P. N. RAMA RAO

Atomic Energy Establishment Trombay, Bombay, India

(Received 22 May 1964; revised manuscript received 6 August 1964)

The kinetic-energy distributions and the correlation of the angular anisotropy and the mass asymmetry of the fission fragments have been determined in the fission of U^{235} induced by 4-MeV neutrons. The kinetic energies of the pair of fragments emitted parallel and perpendicular to the incident beam direction are measured by solid-state detectors and recorded by a three-dimensional analog-to-digital converter incorporating a printout arrangement. The observed variation of the total kinetic energy \bar{E}_k and the mean-square deviation σ_{EK}^2 are found to be different from that observed for the case of thermal fission. For the near-symmetric fragments the total-kinetic-energy distributions show a small peak at an energy of about 125 MeV in addition to the main peak at 163 MeV. The anisotropy has been found to increase with the asymmetry in the region of mass ratios 1.2 to 1.7. The different possibilities leading to the observed dependence of the anisotropy on the asymmetry are discussed.

I. INTRODUCTION

TO understand the mechanism of the mass division in fission, it is important to know whether the mass division depends on the quantum state of the fissioning nucleus at the saddle point. This dependence can be determined by a study of the correlation of the angular anisotropy and the mass asymmetry of the fission fragments, since the work of many authors¹⁻⁵ has shown that the angular distributions of the fission fragments are consistent with the Bohr model⁶ of definite saddle-point states. The anisotropy has been observed to be related to the asymmetry in the case of photofission⁷ of Th^{232} , charged-particle-induced fission⁸ of Th^{232} and 14.9-MeV neutron-induced fission⁹ of U^{238} . However, in all these cases the observed connection between the anisotropy and the asymmetry could arise because of fission taking place at various excitation energies due to the evaporation of neutrons, and therefore, these observations are not sufficient to show any inherent dependence.¹⁰ The direct dependence can be determined in the study of the fission of the compound nucleus excited below the binding energy of a neutron, so that fission takes place only at a single excitation energy.

In the experiments reported here, the relation

between the anisotropy and the asymmetry has been studied in the fission of U^{235} induced by 4-MeV neutrons. The kinetic energies of the pair of fragments emitted nearly along and perpendicular to the direction of the incident beam are measured by back-to-back solid-state detector systems and recorded by a three-dimensional analog-to-digital converter. The data have been analyzed to obtain the distributions in the mass and the total kinetic energy of the fragments emitted at angles of 0 and 90° with respect to the direction of the incident beam. The results show that the angular anisotropy depends on the mass asymmetry of the fragments. The observed variation of the total kinetic energy with the mass ratio is also discussed.

II. EXPERIMENTAL ARRANGEMENT AND METHOD

A schematic diagram of the experimental arrangement is shown in Fig. 1. Neutrons were produced by the $T(p,n)He^3$ reaction using the 5.5-MeV Van de Graaff generator. The maximum energy of the neutrons was about 4.2 MeV, and the spread in the energy of the neutrons due to the slowing down of the protons in the target and the divergence of the neutron beam was estimated to be about 200 keV. The uranium target was prepared by electro-spraying about 300 μg of U^{235} over an area of 1 sq cm on to a VYNS foil coated with a thin layer of gold. The thickness of the VYNS foil and the gold layer was estimated to be about 10 and 15 $\mu\text{g}/\text{cm}^2$ respectively. The uranium foil and three identical solid-state detectors of the diffused-junction type were mounted inside a vacuum chamber (Fig. 1). Each detector had a resistivity of 5500 $\Omega\text{-cm}$, window thickness of less than 1 μ of silicon, and a sensitive depth of about 160 μ , and was operated with 50 V reversed bias. The distance between the surface of one of the detectors (referred to as common detector) and the foil was about 0.2 cm so that most of the fragments emitted in the backward hemisphere were detected by it. At each of the angles of 0 and 90° with the incident direction the

¹ I. Halpern and V. M. Strutinskii, *Proceedings of the International Conference on Peaceful Uses of Atomic Energy* (United Nations, Geneva, 1958), Vol. 15, p. 408.

² J. J. Griffin, *Phys. Rev.* **116**, 107 (1959).

³ R. B. Leachman and E. E. Sanmann, *Ann. Phys. (N. Y.)* **18**, 274 (1962).

⁴ J. E. Simmons and R. L. Henkel, *Phys. Rev.* **120**, 198 (1960).

⁵ R. Chaudhry, R. Vandenbosch, and J. R. Huizenga, *Phys. Rev.* **126**, 220 (1962).

⁶ A. Bohr, *Proceedings of the International Conference on Peaceful Uses of Atomic Energy, Geneva, 1955* (United Nations, New York, 1956), Vol. 2, p. 151.

⁷ A. W. Fairhall, I. Halpern, and E. J. Winhold, *Phys. Rev.* **94**, 733 (1954).

⁸ B. L. Cohen, W. H. Jones, G. H. McCormick, and B. L. Ferrell, *Phys. Rev.* **94**, 625 (1954).

⁹ A. N. Protopopov and O. P. Eismont, *Atomnaya Energiya* **6**, 644 (1959) [English transl.: *Soviet J. At. Energy*, **6**, 475 (1960)].

¹⁰ I. Halpern, *Ann. Rev. Nucl. Sci.* **9**, 245 (1959).

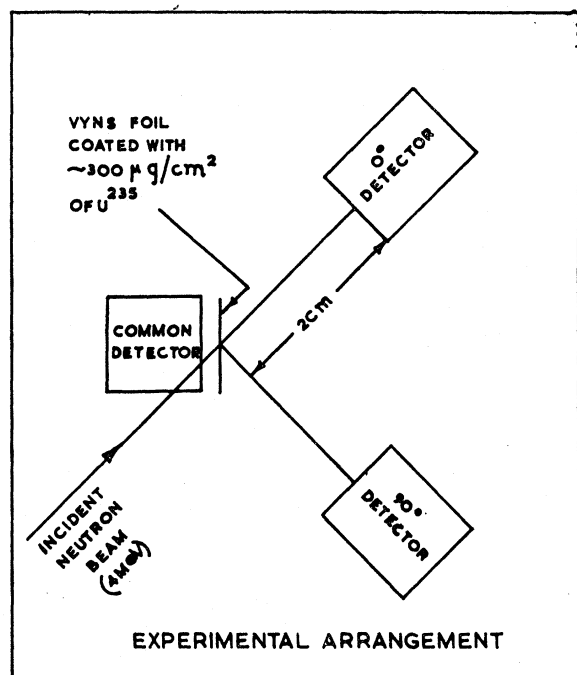


FIG. 1. Schematic diagram of the experimental arrangement.

fragments were detected with an angular spread of about $\pm 18^\circ$. The divergence of the incident neutron beam was calculated to be approximately 3° . The neutron flux at the uranium target was about 6×10^5 neutrons/cm²/sec. The number of fission fragments detected by the common detector was about 40/min, and that detected by each of the 0 and 90° detectors was about 3/min.

Identical charge-sensitive preamplifier-amplifier systems were used for amplifying pulses from the detectors. The coincidence between the pulses from the 0° detector and the common detector (or the 90° detector and the common detector) was used to gate the detector outputs. The gated output pulses were fed to three analog-to-digital converters (ADC) each one employing a Wilkinson gate and an 83.3-kc/sec crystal-controlled subharmonic oscillator. The ADC systems were followed by an automatic printout arrangement which printed the three numbers separately. If a fragment was detected by the 0° detector, the number corresponding to the 90° detector was zero and vice versa. The output pulse heights were transformed into energies by a calibration of each of the detector systems using the kinetic energy distribution for the thermal fission of U²³⁵ as obtained by the time of flight technique.¹¹ To compare the kinetic energy distribution obtained by the solid-state detector to that obtained by the time-of-flight method, the latter was corrected¹² to represent the kinetic-energy distribution after neutron emission.

¹¹ J. C. D. Milton and J. S. Fraser, *Can. J. Phys.* **40**, 1626 (1962).

¹² H. C. Britt and H. E. Wegner, *Rev. Sci. Instr.* **34**, 274 (1963).

As the peak positions in the kinetic-energy distribution of single fragments are nearly the same^{13,14} for the fission induced by thermal neutrons and by medium energy neutrons, the above calibration procedure is justified. The fragment masses were calculated using the momentum conservation relation $M_L E_L = M_H E_H$ where M_L , E_L , and M_H , E_H are the mass and the kinetic energy for the light and the heavy fragments respectively. The data were analyzed using the computer TIFRAC.

The total number of runs carried out over a period of 20 days was 15. To ensure the stability of the calibration of the detector systems and the associated electronics, checks were made at the end of each run and the data were analyzed separately for each run. The total number of events recorded both in the 0 and 90° directions was about 40 000. The counts $N(0^\circ)$ and $N(90^\circ)$, from the 0 and 90° detectors respectively, were also separately monitored to determine the anisotropy of the fragments.

III. EXPERIMENTAL RESULTS

The ratio $N(0^\circ)/N(90^\circ)$ as determined from the monitor counts of the 0 and 90° detectors has been found to be equal to 1.15 ± 0.03 . This value, uncorrected for geometrical resolution, compares favorably with the value of 1.13 ± 0.020 obtained by Simmons and Henkel,⁴ and of 1.18 ± 0.02 obtained by Leachman and Blumberg.¹⁵ From the calculated mass distributions, the following results are obtained

$$N_L(0^\circ)/N_H(0^\circ) = 1.01 \pm 0.01;$$

$$N_L(90^\circ)/N_H(90^\circ) = 0.99 \pm 0.01,$$

where N_L and N_H are the total number of the light and the heavy fragments, respectively. It can be seen that within the statistical accuracy of one percent the numbers of the light and heavy fragments emitted in the 0° direction are equal. This shows that the angular distributions are symmetric about 90° implying that the light and the heavy fragments have identical angular distributions. This is in agreement with the results of the previous work^{9,16-18} but in disagreement with the work of Brolley *et al.*¹⁹ on the fission of Np²³⁷ by 14.3-MeV neutrons where the light and the heavy fragments were found to have different angular distributions.

¹³ J. S. Wahl, *Phys. Rev.* **95**, 126 (1954).

¹⁴ Yu. A. Blyumkina, I. I. Bondarenko, V. F. Kuznetsov, V. G. Nesterov, V. N. Okolovitch, G. N. Smirenkin, and L. N. Usachev, *Nucl. Phys.* **52**, 648 (1964).

¹⁵ R. B. Leachman and L. Blumberg (to be published).

¹⁶ B. Cohen, B. Ferrell-Bryan, D. Coombe, and M. Hullings, *Phys. Rev.* **98**, 685 (1955).

¹⁷ R. B. Leachman and G. P. Ford, *Nucl. Phys.* **19**, 366 (1960).

¹⁸ I. A. Baranov, A. N. Protopopov, and V. P. Eismont, *Zh. Eksperim. i Teor. Fiz.* **41**, 1003 (1961) [English transl.: *Soviet Phys.—JETP* **14**, 713 (1962)].

¹⁹ J. Brolley, W. Dickinson, and R. Henkel, *Phys. Rev.* **99**, 159 (1955).

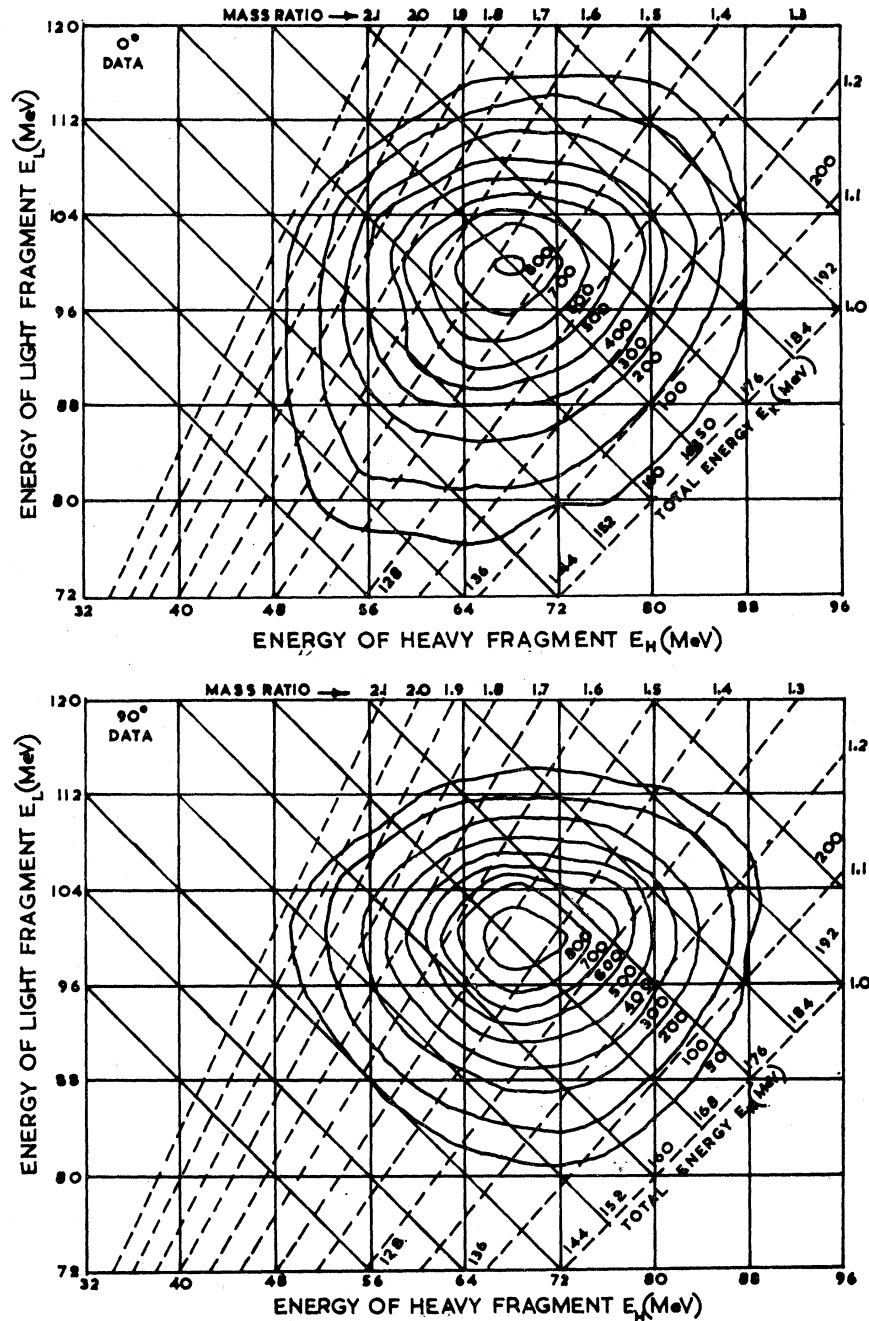


FIG. 2. Contour plots of the data for the 4-MeV neutron-induced fission of U^{235} in the cases when the fragments are emitted (a) parallel, and (b) perpendicular to the incident beam direction. The number labeling each contour represents the frequency of occurrence of the events defined by the contour. The total number of events are about 4×10^4 .

The results of the measurements are summarized compactly in the contour plots of Figs. 2(a) and 2(b) which have been drawn from the E_L-E_H matrix by interpolations between two points and represent the probability distribution $N(E_L, E_H)$. The number labeled on each of the contours gives the relative frequency of occurrence of the events defined by the contour. The mass distributions of the fragments emitted at angles of 0 and 90° to the incident beam, as obtained from the analysis of the data, are shown in Fig. 3(a). These

distributions have been corrected for the systematic effects of the emission of neutrons as described by Terrell²⁰ and Britt *et al.*²¹ The error ΔM_H in the calculated mass M_H is given by

$$\Delta M_H = M_H - M_H^* = \{ \nu_H - [M_H^* \nu_T / (M_H^* + M_L^*)] \}, \quad (1)$$

²⁰ J. Terrell, Phys. Rev. **127**, 880 (1962).

²¹ H. C. Britt, H. E. Wegner, and S. L. Whetstone, Jr., Nucl. Instr. Methods **24**, 13 (1963).

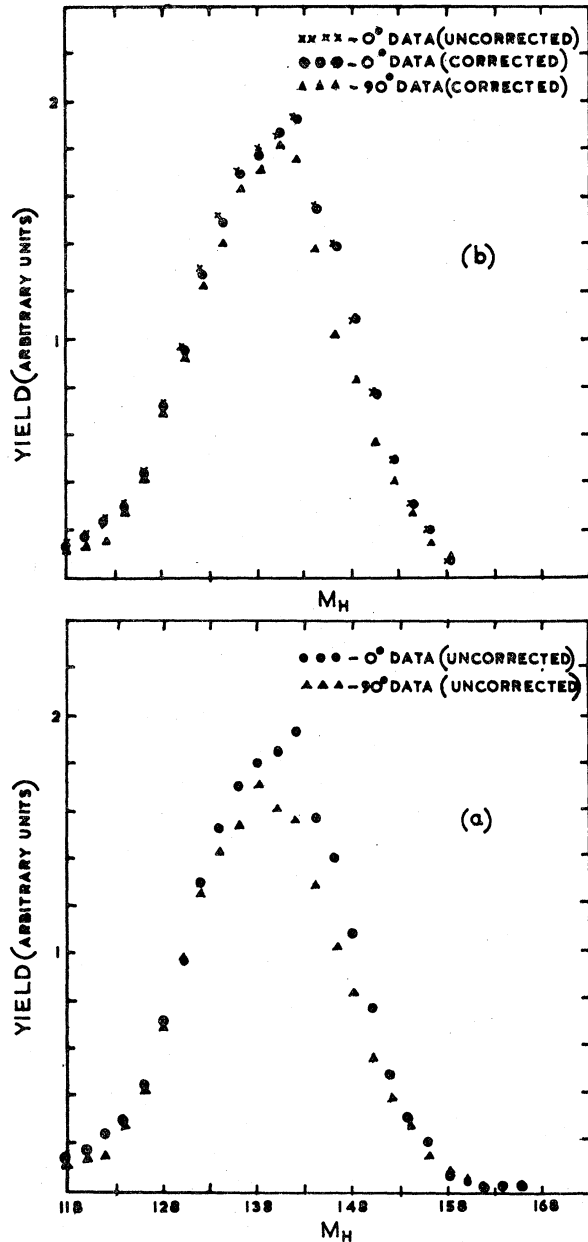


FIG. 3. (a) Mass yields of the fragments emitted in the 0 and 90° directions plotted against the heavy fragment mass. These distributions are the observed yields uncorrected for the effects of the neutron emission. (b) Mass yields of the fragments emitted in the 0 and 90° directions plotted against the heavy fragment mass after correcting for the systematic effects of the neutron emission on the assumption that the pair-fragments emit equal number of neutrons. For comparison, the uncorrected mass yield of the 0° fragments is also shown as crossed points.

where M_H^* , M_L^* are the corrected masses of the light and heavy fragments, respectively, and ν_H and ν_T are the number of neutrons emitted from the fragment of mass M_H and the total number of neutrons from both fragments, respectively.

The variation of ν_T with the fragment mass division

was calculated using the measured values of the total kinetic energy \bar{E}_k for each mass division, on the energy-balance considerations, as described later. Since there exists no information on the variation of number of neutrons with the fragment mass in the case of the fission of U^{235} by 4-MeV neutrons by direct measurements, it was assumed that $\nu_L = \nu_H = \nu_T/2$. This assumption may not be fully justified at medium excitation energies, especially in the region of the symmetric mass divisions. As the corrected values appear to be closely dependent on the nature of the variation of $\nu(M)$, the applied corrections can be considered only approximate. The corrected distributions are shown in Fig. 3(b). For comparison, the uncorrected mass distribution of the fragments emitted in the 0° direction is also shown in the same figure. The values \bar{M}_H of the average heavy fragment mass are found to be (139.0 ± 0.2) and (138.6 ± 0.2) for the fragments emitted in the 0 and 90° directions respectively. The variances σ_M^2 of the observed mass distributions for the 0 and 90° fragments are found to be same and equal to 65.3. The value of the variance for both the mass distributions obtained after correcting only for the systematic effects of neutron emission is 61.9. This latter value includes a variance of about 2.0 due to the dispersion²⁰ resulting from the varying directions and number of emitted neutrons, an estimated variance of about 0.8 due to the experimental energy resolution of the semiconductor detectors, and a variance of about 1.0 due to the spread introduced by the thickness of the uranium foil. The estimated variance due to the neutron spread effect is approximate because of the assumption that $\nu_L = \nu_H = \nu_T/2$. The estimate of the spread introduced by the uranium target is also approximate owing to the possible nonuniformity in the coating of uranium target. Further, the target thickness affects the yield of the near symmetric fragments resulting in a lower peak-to-valley ratio. However, all the above dispersions are expected to be the same for the 0 and 90° mass distributions in the geometry employed, and will cancel out if the comparison of these two mass distributions is involved. The 0 and 90° detector systems were found to give identical kinetic energy and mass distributions of the fission fragments in the case of the thermal neutron induced fission of U^{235} , thus ensuring identical responses of the two detector systems. The effect of the center-of-mass motion on the mass distribution in the 0° direction was estimated and was found to be insignificantly small.

The anisotropy $\{N(0^\circ)/N(90^\circ)\}$ for the various mass ratios as calculated from Fig. 3 is shown in Fig. 4. This plot is independent of the effects of the neutron emission on the mass distributions, if it is assumed that the characteristics of the neutron emission are the same for emission from the fragments emitted along the 0 and 90° directions. The variation of the average kinetic energy with the fragment mass ratios for the two cases as observed in the present experiment supports this

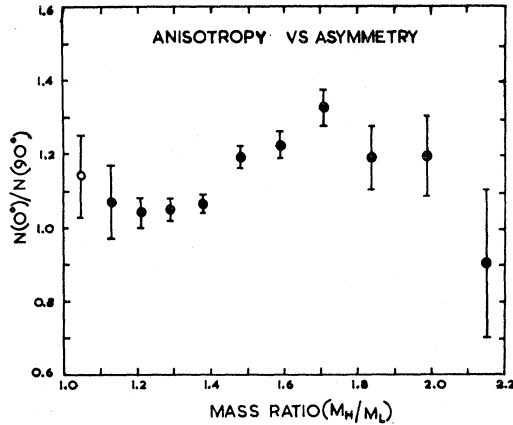


FIG. 4. Angular anisotropy $\{N(0^\circ)/N(90^\circ)\}$ versus mass asymmetry (M_H/M_L) calculated from the observed mass yields shown in Fig. 3 (a).

assumption. From Fig. 4 it is seen that the anisotropy increases with the mass ratio in the region of mass ratios between 1.2 to 1.7. Further, in the regions of lesser statistical accuracy the anisotropy seems to decrease for mass ratios greater than 1.7 and to increase for mass ratios lesser than 1.2. Earlier measurements by Baranov *et al.*¹⁸ for the fission of U^{238} by 3-MeV neutrons using a double ionization chamber do not show the increase in the anisotropy between the mass ratios of 1.25 and 1.65, but the anisotropy was found to be higher for the mass ratio of 1.0 than for 1.25. The variance σ_M^2 of the mass distributions obtained by Baranov *et al.*¹⁸ is about 85, which is significantly higher than the value obtained in the present work. This shows that the mass resolution obtained in their work is poorer, probably because of the use of a thicker source and gridded ionization chamber as compared to solid-state detectors. This might have been responsible for masking the dependence of the anisotropy on the asymmetry in their experiment. A larger anisotropy for the symmetric fragment group was also found by Manley²² in the study of fission of U^{238} induced by neutrons of energy from 1.2 to 1.7 MeV, using the photographic emulsion technique, but the mass resolution in this work is not sufficient to obtain detailed information about the variation of the anisotropy with the asymmetry.

The average total kinetic energies of the fragments and the rms deviations of the distributions are found to be as follows:

$$\begin{aligned}\bar{E}_k(0^\circ) &= (165.4 \pm 1.1) \text{ MeV}; \\ \bar{E}_k(90^\circ) &= (166.0 \pm 1.1) \text{ MeV}; \\ \sigma_{E_k}(0^\circ) &= (11.70 \pm 0.06) \text{ MeV}; \\ \sigma_{E_k}(90^\circ) &= (10.85 \pm 0.06) \text{ MeV}.\end{aligned}$$

The variation of the average total kinetic energy \bar{E}_k with the fragment mass ratio after correcting for the

effects of neutron emission is shown in Fig. 5(a) along with that for the case of thermal fission.¹¹ The events shown in the symmetric region of mass ratios between 1.0 and 1.1 have a significant contribution from the regions of the higher mass ratios owing primarily to the target thickness effects. Hence the values of \bar{E}_k , $\sigma_{E_k}^2$ and other parameters determined in this region (shown by open points) do not exactly correspond to the mass ratios indicated. However, the trend of variation of \bar{E}_k does show a significantly larger value of \bar{E}_k at symmetry as compared to the value in the thermal fission. For the calculation of the correction ΔE_k to the measured total kinetic energy \bar{E}_k the following approximate expression²¹ was used:

$$\Delta E_k = \{\bar{E}_k / (A - \nu_T)\} \{\nu_L R + (\nu_H / R)\}, \quad (2)$$

where $R = (M_H/M_L)$. The correction to the measured

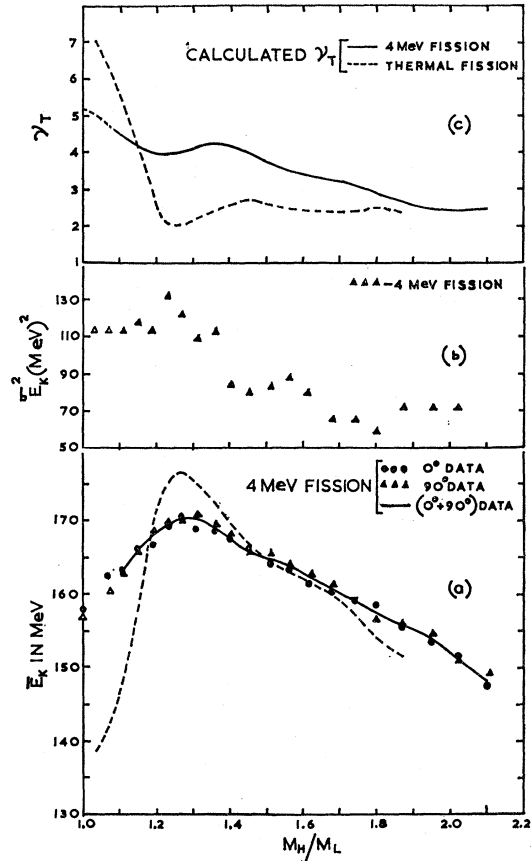


FIG. 5. (a) Plot of the average total kinetic energy \bar{E}_k of the fragments against mass ratios. The values of \bar{E}_k have been corrected for the effects of neutron emission. The observed variation of \bar{E}_k with the fragment mass ratios, as observed (Ref. 11) in the thermal neutron fission of U^{235} , is also shown. (b) The variance $\sigma_{E_k}^2$ of the total kinetic energy of E_k of the fragments plotted against fragment mass ratios for the 90° data. (c) Total number ν_T of the neutrons emitted for the various mass divisions as calculated on the energy balance considerations using the measured values of \bar{E}_k . In the data for the 4-MeV neutron-induced fission in the region of mass ratios 1.0 to 1.1 (shown by dotted line) there is a significant contribution from the higher mass ratios.

²² J. H. Manley, Nucl. Phys. 33, 70 (1962).

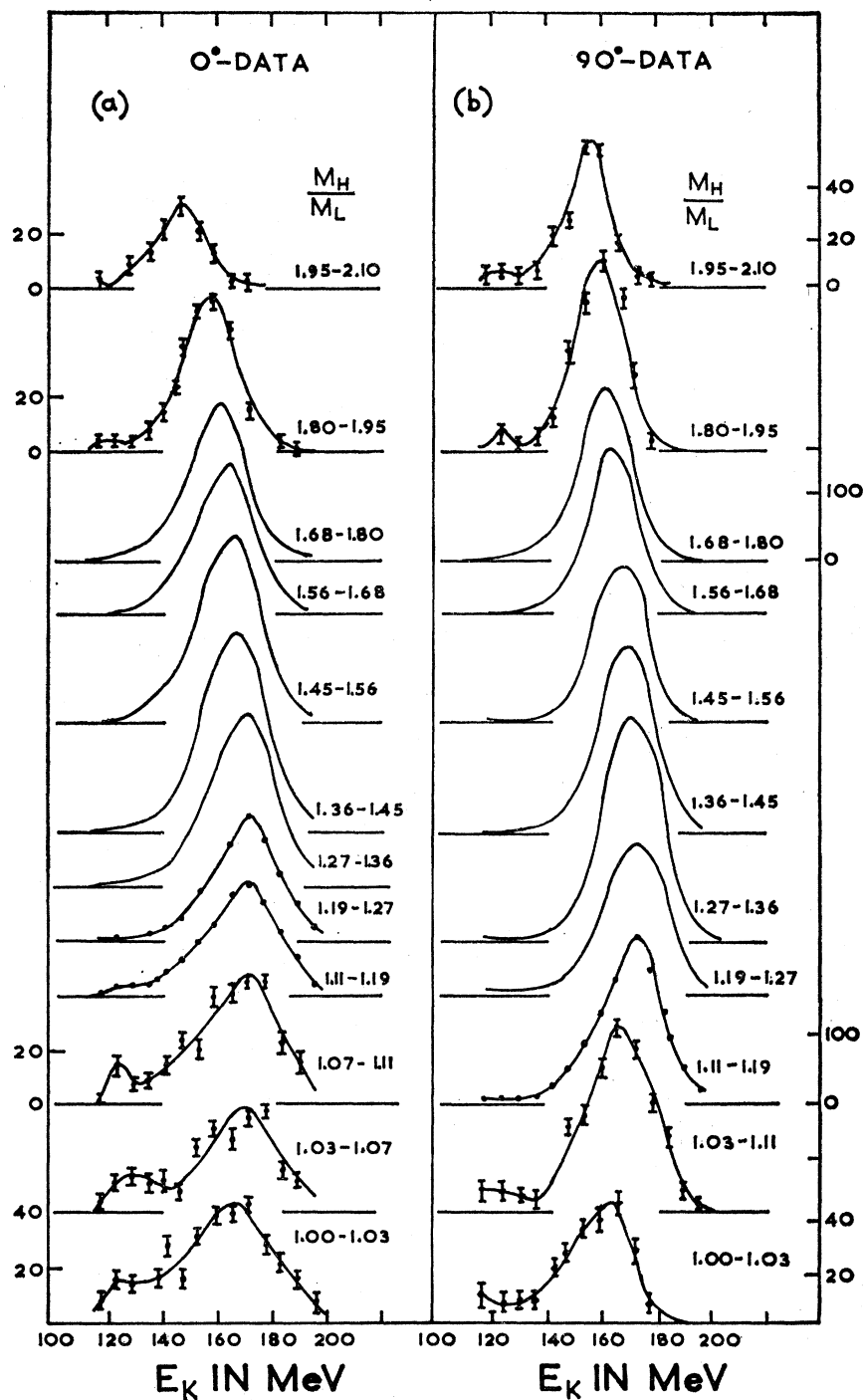


FIG. 6. (a) The total kinetic energy distributions for the various fragment mass ratios for the 0° data. (b) The total kinetic energy distribution for the various fragment mass ratios for the 90° data.

values of \bar{E}_k has been applied on the assumption of $\nu_L = \nu_H = \nu_T/2$.

The calculated error ΔE_k is only weakly dependent on the nature of variation of $\nu(M)$ and therefore, the errors in the values ΔE_k calculated on the assumption of $\nu_L = \nu_H = \nu_T/2$ are very small. From the observed values of \bar{E}_k , uncorrected for the neutron emission

effects, the total number of neutrons ν_T emitted for each mass ratio is calculated on the energy balance consideration, and are shown in Fig. 5(c). However, the values of ΔE_k are not appreciably changed if the corrected values of \bar{E}_k are used in the calculations. In these calculations, the values of the energy released and the neutron binding energies have been taken from

Milton,²³ and it has been assumed that for each mass division the average energy emitted as gamma rays is 7.5 MeV and the average emission energy of the neutrons is 1.2 MeV. It can be seen from Fig. 5(a) that the variation of \bar{E}_k with the fragment mass ratios is nearly the same for the fragments emitted parallel and perpendicular to the incident neutron beam, indicating that the characteristics of the neutron emission for various mass ratios are the same for the two cases. The variation of the mean-square deviations $\sigma_{E_k}^2$ of the total kinetic-energy distributions with the mass ratios for the 90° data is shown in Fig. 5(b). A similar variation of $\sigma_{E_k}^2$ has been found for the 0° data. The observed variation of $\sigma_{E_k}^2$ is different from that observed by Milton and Fraser¹¹ for the thermal fission of U^{235} but agrees with recent experiments²⁴ in the medium energy fission and the trend calculated by Fong.²⁵

Figures 6(a) and (b) show the distributions in the total kinetic energy of the fragments emitted at angles of 0 and 90° with the incident neutron direction, for the various fragment mass ratios. An interesting feature of the distribution in the region of the fragment mass ratios of 1.00 to 1.11 is the appearance of a second small peak at an energy of about 125 MeV in addition to the main peak at about 163 MeV. This feature is more pronounced in the case of the 0° distributions. For the fragment mass ratios higher than 1.11, the low-energy peak disappears, with an indication of a similar small peak at an energy of about 120 MeV appearing again for the very asymmetric fragments. Komar *et al.*²⁶ have reported similar double-peaked distributions for the total kinetic energy of the near symmetric fragments in the case of fission of Th^{232} induced by 14-MeV neutrons.

IV. DISCUSSION

(A) Kinetic-Energy Distributions

The average separation of the effective charge centers at the scission point for the various mass divisions can be obtained from the measured variation of \bar{E}_k with fragment mass ratios as the kinetic energy arises from the Coulomb repulsion between the fragments at scission. The elongation of the fissioning nucleus at scission for the various mass divisions can be expressed in terms of a parameter β which can be defined as the ratio of the actual distance between the charge centers to the distance if the fragments were formed spherical, and is given by the relation

$$\beta = \{Z_L^p Z_H^p e^2\} / \{\bar{E}_k r_0 (A_L^{1/3} + A_H^{1/3})\}, \quad (3)$$

²³ J. C. D. Milton, University of California Radiation Laboratory Report UCRL-9883, Rev. 1962 (unpublished).

²⁴ H. C. Britt and S. L. Whetstone, Jr., *Phys. Rev.* **133**, B603 (1964).

²⁵ P. Fong, Argonne National Laboratory Report No. ANL 6797, 1963, p. 416 (unpublished).

²⁶ A. P. Komar, B. A. Bochagov, and V. I. Fadeev, *Dokl. Akad. Nauk SSR* **152**, 858 (1963) [English transl.: *Soviet Phys.—Doklady* **8**, 978 (1964)].

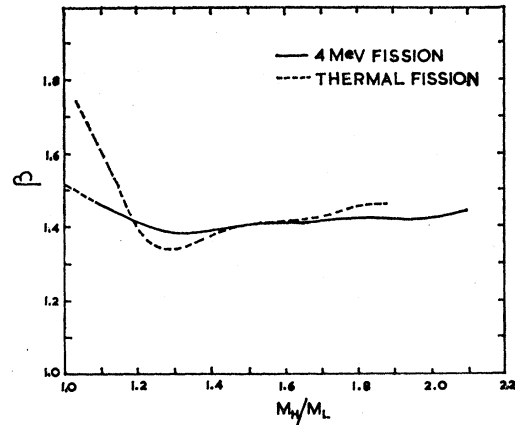


FIG. 7. Variation of the calculated β with the fragment mass ratios for the thermal and 4-MeV neutron-induced fission of U^{235} . β is the ratio of the actual distance between the effective charge centers of the fragments at the scission point to the distance if the fragments were formed spherical. In the data for the 4-MeV neutron-induced fission in the region of mass ratios 1.0 to 1.1 (shown by dashed line) there is a significant contribution from the higher mass ratios.

where Z_L^p , Z_H^p are the most probable charges for the fragments of mass numbers A_L and A_H , respectively. The values of β calculated for different mass ratios, using the measured values of \bar{E}_k and the tabulated values²³ of Z_L^p and Z_H^p , are shown in Fig. 7 for thermal and 4-MeV neutron-induced fission.

For thermal fission the occurrence of the minimum value of β at the mass ratio of 1.27 can be explained by the shell effects, as the heavy fragment in this case is doubly magic. A value of β in the region of mass ratios 1.19 to 1.48 for the case of 4-MeV neutron-induced fission higher than for thermal fission signifies that the shell effects are less predominant at higher excitation energies. For all the other mass divisions, the value of β is higher for the thermal fission than for the 4-MeV neutron-induced fission, showing that at higher excitation energies the nucleus undergoes less stretching up to the scission, indicating that the "tensile strength" of the nucleus decreases with the increase in the excitation energy. The largest difference in the values of β for the two cases, occurs in the case of symmetric fragments, showing that the symmetric fragments are formed in a significantly more stretched configuration in the thermal fission. For this reason, the symmetric fragments produced in the thermal fission emit more neutrons than those produced in the medium energy induced fission [Fig. 5(c)]. These differences in the characteristics of the symmetric fragments with regard to their kinetic and excitation energy suggests that these are produced by different mechanisms in the two cases. Further evidence of the existence of the two different mechanisms can be drawn from the observation of the presence of the small low-energy peak in the total kinetic-energy distribution for the near symmetric region [Figs. 6(a) and 6(b)].

(B) Anisotropy versus Asymmetry

It has been shown by several workers¹⁻⁵ that the measurements of the angular distribution of the fission fragments are consistent with the predictions of the Bohr model⁶ of definite saddle-point states. On the basis of this model a dependence of the anisotropy on the asymmetry can arise if the final mass division depends on the saddle-point shapes and each saddle-point shape has a different sequence of the quantum numbers. From the results of the present experiment, a dependence of the final mass division on the saddle-point shapes, in at least the medium energy induced fission, can therefore be inferred. The dependence of the saddle-point quantum numbers on the different shapes can arise for various reasons. On the basis of the analysis of Halpern and Strutinski¹ and Griffin,² the anisotropy increases with the decrease in the value of K_0^2 , where K_0^2 is the mean square of the projection of the total angular momentum \mathbf{I} on the nuclear symmetry axis. On statistical arguments it has been shown that

$$K_0^2 = J_{\text{eff}}T/\hbar^2 = \text{const}J_{\text{eff}}(E_{\text{ex}} - E_{\text{th}})^{1/2}/\hbar^2, \quad (4)$$

where J_{eff} and T are the effective moment of inertia and the nuclear temperature respectively of the nucleus at the saddle point. E_{ex} is the initial excitation energy of the nucleus and E_{th} is the fission threshold which is equal to the deformation energy at the saddle point. The observed correlation can, therefore, be associated either with the variation of J_{eff} or T or both with the saddle-point shape of the nucleus. However, the

evaluation of J_{eff} for the various mass divisions requires a detailed knowledge of the corresponding saddle-point shapes about which at present very little is known. The observed increase in the anisotropy with the asymmetry in the region of the mass ratios 1.2-1.7 implies that the product $J_{\text{eff}}T$ decreases with the increase in the mass ratio. At about 5-MeV excitation energy of the uranium nucleus and for the distortions which occur at the saddle point, the moment of inertia of the nucleus is probably close to the rigid body value. It has been shown⁵ that for rigid body rotations, J_{eff} decreases with the increasing distortion at the saddle point. Both J_{eff} and T will, therefore, separately decrease, if E_{th} increases in this region of the mass ratios. Hence, the observed variation of the anisotropy, implies that the saddle point deformation energy E_{th} increases with the asymmetry in the saddle-point shape in the region of mass ratios 1.2 to 1.7.

The purpose of the present discussion on the observed variation of the anisotropy with the asymmetry has only been to point out the various possibilities leading to the observed dependence. A quantitative estimate of the various factors affecting the dependence of the anisotropy for the various saddle point shapes is necessary for more detailed discussion.

ACKNOWLEDGMENTS

Our thanks are due to S. R. S. Murthy, B. R. Ballal, and S. L. Raote for their help in carrying out the experiment and for making several electronic units. We are thankful to K. S. Kane for his help in carrying out the computer program.